The trends in reactivity for ion-bombarded GaAs exposed to various gases[4] (reactivity NO > O_2 > N_2O) are very similar to the results reported by others[1,2,5,8] for photoenhanced chemical reactions on GaAs. Both O_2 and NO exhibit photoenhancement reaction[1,2,6,8] with GaAs, whereas N_2O does not exhibit photoenhancement.[1] Photon-induced enhancement in reactivity is attributed to interaction of the adsorbed molecule with photogenerated carriers, i.e., electron–hole pairs that are created in the bulk by interaction of the photon with the semiconductor. The pairs migrate to the surface and react with the adsorbate–surface complex and induce reactions.[20] Photoenhanced reactions involve the interaction of the adsorbing species with an increased concentration of electrons at the surface. As a result of the present study, it is suggested that processes for ion-bombarded GaAs may be similar to those occurring in photoenhanced reactions where ion-bombardment generated singly occupied gallium orbitals (free electrons) and other defects are principal active sites for reactions with gases.

The differences in the extent of oxidation for Xe^+ and Ne^+ ion-bombarded GaAs surfaces by either NO, O_2, or N_2O support previous results[4] where the effect of the mass of the bombarding ion on the chemical reactivity was investigated. Damage caused by Xe^+-ion bombardment is confined mainly to surface atoms, therefore imparting more defects at the surface. The penetration of Ne^+ into GaAs is greater than for Xe^+, and thus fewer defects are found at the surface. Hence, the concentration of defects at the surface is greater following Xe^+ bombardment, and thus Xe^+-ion-bombarded GaAs exhibits increased relative reactivity for all three gases.

Acknowledgment. We acknowledge the funding of this project by Texas Instruments and the Virginia Center for Innovative Technology. The National Science Foundation provided funds for an equipment grant.

Registry No. GaAs, 1303-00-0; N_2O, 10024-97-2; NO, 10102-43-9; O, 7782-44-7; Ne^+, 14782-23-1; Xe^+, 24203-25-6.

(20) Ying, Z.; Ho, W. *Phys. Rev. Lett.* **1988**, *60*, 57.

$Ca_4Bi_6O_{13}$, a Compound Containing an Unusually Low Bismuth Coordination Number and Short Bi···Bi Contacts

J. B. Parise,*,† C. C. Torardi,*,‡ M.-H. Whangbo,*,§ C. J. Rawn,⊥ R. S. Roth,*,⊥ and B. P. Burton⊥

Mineral Physics Institute, Department of Earth and Space Sciences, State University of New York, StonyBrook, New York 11794; Central Research and Development Department, E. I. du Pont de Nemours and Co., Inc., Experimental Station, Wilmington, Delaware 19880; Department of Chemistry, North Carolina State University, Raleigh, North Carolina 27695; and National Institute of Standards and Technology, Gaithersburg, Maryland 20899

Received February 12, 1990

Single crystals and powder samples of a new bismuth(III) calcium oxide, $Ca_4Bi_6O_{13}$, have been synthesized and studied by X-ray diffraction. This compound crystallizes in the orthorhombic space group $C2mm$ with $Z = 2$. The absence of a center of symmetry was confirmed by the presence of a second harmonic signal some 60 times that observed for quartz. The cell parameters are $a = 5.937$ (1), $b = 17.356$ (4), $c = 7.206$ (4) Å. A weak superstructure (2 × 3.6 Å), visible in long-exposure rotation and precession photographs, exists along c^* due in part to alternation of oxygen and vacancies along the c axial direction. The structure consists of ribbons of edge-linked BiO_5 square pyramids running parallel with the c axis. These chains are linked via a novel three-coordinate Bi atom to form semicylinders stacked along the a axial direction. Sheets of these units are then stacked along the b axial direction and are separated by Ca ions in 7-fold coordination with oxygen. Along the c direction, the three-coordinate Bi atoms form ···BiOBi···BiOBi··· chains. The Bi···Bi contacts of these chains are short, 3.341 (2) Å, and the bridging oxygen atoms are displaced by about 0.25 Å from the centers of the Bi–O–Bi bridges in the direction perpendicular to these bridges. Molecular orbital calculations suggest that this displacement of the bridging oxygen atoms reduces the extent of lone pair–lone pair repulsion that occurs in each short Bi···Bi contact.

Introduction

The frenetic activity devoted to determination of the structural properties of the alkali metal/bismuth oxide/copper oxide based superconductors has somewhat overshadowed a need for a better understanding of the phase relations in the binary and ternary oxide systems on which they are based. As part of an ongoing study of the structural characterization of compounds in these systems,[1] we report here the structure of $Ca_4Bi_6O_{13}$. With respect to copper-containing superconductors, we were particularly interested in obtaining precise information on the geometric nature of the Bi coordination, a topic of some discussion in the literature.[2-5] In $Ca_4Bi_6O_{13}$ the bismuth

† State University of New York.
‡ E. I. du Pont de Nemours and Co.
§ North Carolina State University.
⊥ National Institute of Standards and Technology.

(1) (a) Roth, R. S.; Rawn, C. J.; Ritter, J. J.; Burton, B. P. *J. Am. Ceram. Soc.* **1989**, *72*, 1545. (b) Roth, R. S.; Rawn, C. J.; Bendersky, L. A. *J. Mater. Res.* **1990**, *5*, 46. (c) Hwang, N. M.; Roth, R. S.; Rawn, C. J. *J. Am. Ceram. Soc.*, to be published. (d) Roth, R. S.; Burton, B. P.; Rawn, C. J. *J. Am. Ceram. Soc.*, to be published. (e) Roth, R. S.; Rawn, C. J.; Burton, B. P.; Beech, F. *J. Res. NIST*, to be published. (f) Roth, R. S.; Rawn, C. J.; Burton, B. P.; Beech, F. *Abstr. Am. Crystallogr. Assoc. Ser. 2* **1989** *17*, 41.

0897-4756/90/2802-0454$02.50/0

Table I. Summary of X-ray Diffraction Data for $Ca_4Bi_6O_{13}$

color	pale yellow
size, mm	0.05 × 0.06 × 0.26
cryst syst	orthorhombic
space group	*C2mm* (No. 38)
a, Å	5.937 (1)
b, Å	17.356 (4)
c, Å	7.206 (4)
temp, °C	20
vol, Å^3	742.5
Z	2
formula wt	1622.19
calcd density, g/cm^3	7.255
μ(Mo), cm^{-1}	720.65
diffractometer	Enraf-Nonius CAD4
radiation (graphite monochromator)	Mo Kα
data coll	1202
min, max 2θ, deg	4.7, 60.0
max *h*,*k*,*l*	8 24 10
data octants	+++, −++
scan method	ω
abs method	DIFABS[a]
transm factors, range	0.01–0.03
no. of unique data ($I > 3.0\sigma(I)$)	1077
refinement method	full-matrix least squares on *F*
anomalous dispersion	Bi, Ca
weighting scheme	$\propto[\sigma^2(I) + 0.0009I^2]^{-1/2}$
atoms refined	aniso, Bi, Ca; iso, O
parameters varied	45
data/parameter ratio	23.91
R	0.029 (0.049)[b]
R_w	0.032 (0.059)[b]
error of fit	1.21
secondary extinction coefficient, mm	0.06 (1) × 10^{-4}

[a] Reference 7. [b] Numbers in brackets refer to values for enantiomorph.

atom is found in a variety of coordination geometries, from three to six (5 + 1) coordinate with oxygen. Freed from the strictures imposed by a rigid covalent CuO network in the superconductors,[2] the structure of $Ca_4Bi_6O_{13}$ is relatively well ordered and affords an opportunity to study aspects of Bi geometry and bonding made more difficult in the former compounds.

Experimental Section

Synthesis and Characterization. The compound was synthesized by mixing together $CaCO_3$ and $^1/_2Bi_2O_3$ in the stoichiometric molar ratio of 2:3. The best single-phase material was obtained by successive overnight heat treatments, with intermediate mixing and grinding at 700, 800, 900 and twice at 750 °C. The 900 °C heat treatment converts this compound to the high-temperature body-centered cubic solid solution, and several successive heat treatments at 750 °C are necessary to completely revert the material to the low-temperature polymorph. This phase is the same as that previously reported by Conflant et al.[6] as having the formula $Ca_7Bi_{10}O_{22}$. However, the work of Roth et al.[1c,d] clearly shows that the true ratio of Ca:Bi is 2:3.

The phase equilibria diagram of Conflant et al.[6] and Hwang et al.[1] for the CaO–Bi_2O_3 binary system indicates that the low-temperature polymorph of $Ca_4Bi_6O_{13}$ is not in equilibrium with the liquid at any composition. Therefore, a preequilibrated specimen of CaO:$^1/_2Bi_2O_3$ (7:10) was mixed with a $(Na_{0.5}K_{0.5})Cl$ eutectic salt solid solution in the ratio of charge/flux 20/80. The mixture was heated in a sealed Pt tube at 750 °C and cooled to the solidus temperature of the salt solution, 645 °C, at 1 °C/h. After removing from the furnace, the salt was dissolved in H_2O, and many euhedral crystals of pale yellow color were obtained. The crystals are elongated prisms with ~10:1 aspect ratio, generally terminated on at least one end. The direction of elongation is the one corresponding to the unit cell dimension of ~(3.6 × 2) Å. Optical examination of the crystals under a polarizing microscope showed no evidence of twinning. The crystals were found by the precession method to be orthorhombic, space group *Cmmm* (No. 65), *Cmm2* (No. 35), *C2mm* or *Cm2m* (No. 38), or *C222* (No. 21). The unit cell was reported as *a* = 17.399 (5), *b* = 5.944 (2), *c* = 7.232 (2) Å,[1f] determined from powder X-ray diffraction data (Cu Kα), completely indexed up to 40° in 2θ. Rotation and precession photographs, as well as powder diffractograms, are consistent with the presence of a strong subcell along *c** such that $c^* = {}^1/_2c^*_{subcell}$. This feature of the diffraction geometry was not revealed by the automatic peak search/Bravais lattice selection routine of the single crystal diffractometer used for data collection; careful preliminary photographic reconnaissance was a valuable check in this instance. In addition, the photographic work, consistent with the optical examination, also gave no evidence of twinning.

Structure Determination. Data were collected on an Enraf-Nonius CAD-4 diffractometer using the experimental parameters given in Table I. The cell parameters reported in Table I were determined from 25 reflections with 6° < θ < 23°. The reflections were corrected for Lorentz and polarization effects; absorption corrections were performed by using the program DIFABS following the solution of the structure.[7]

Structure solution was initiated in space group *Cmmm* using a Patterson function peak search/solution algorithm developed by Calabrese.[8] A trial structure derived from the positions of three Bi atoms that best explained the strongest peaks in the Patterson map led to a discrepancy index of 0.12. At this stage a difference map revealed a calcium atom split about the mirror plane in (100). Upon lowering the symmetry to *C2mm*, the discrepancy index improved markedly. By employing an absorption correction[7] and anisotropic thermal parameters for the metal atoms, the final discrepancy indexes reported in Table I were obtained. Values for the refinement of the structure of the enantiomorph are also given. Oxygen atom O(2) appeared to have highly anisotropic thermal motion in the *ab* plane, particularly in the *b* direction, when situated on the 2*b* sites (*x*, 0, $^1/_2$). This indicated a statistically occupied disordered site for O(2). A significant improvement in the *R* factors and isotropic thermal

Table II. Fractional Coordinates and Isotropic Thermal Parameters for $Ca_4Bi_6O_{13}$

atom	site[a]	*x*	*y*	*z*	U,[b] Å
Bi(1)	4d	0.0 (0)	0.11236 (3)	0.0 (0)	5.1 (3)′
Bi(2)	4e	0.49000 (16)	0.38906 (3)	0.5 (0)	3.8 (3)′
Bi(3)	4c	0.01355 (18)	0.5 (0)	0.76819 (7)	6.3 (2)′
Ca(1)	8f	0.9415 (4)	0.2861 (1)	0.7477 (3)	5.8 (9)′
O(1)	4d	0.1435 (18)	0.2201 (7)	0.0 (0)	5 (3)
O(2)	4e (2b)[c]	0.0991 (36)	0.5140 (2)	0.5 (0)	15 (5)
O(3)	4e	0.6565 (18)	0.2835 (7)	0.5 (0)	6 (3)
O(4)	8f	0.2638 (13)	0.3473 (5)	0.7422 (10)	13 (1)
O(5)	8f	0.7842 (14)	0.4107 (5)	0.7624 (11)	16 (1)

[a] Space group *C2mm* (No. 38). [b] Metal atoms refined with anisotropic thermal parameters, U_{equiv} (Å × 1000) is shown. [c] Atom displaced from 2b site to half-occupied 4e sites.

Table III. Anisotropic Thermal Parameters[a] (Å × 1000) for the Metal Atoms of $Ca_4Bi_6O_{13}$

atom	U_{11}	U_{22}	U_{33}	U_{12}	U_{13}	U_{23}
Bi(1)	3.9 (4)	4.1 (2)	5.5 (2)	−1.4 (3)	0.0 (0)	0.0 (0)
Bi(2)	4.1 (4)	3.2 (2)	4.6 (2)	0.9 (3)	0.0 (0)	0.0 (0)
Bi(3)	5.5 (3)	9.2 (2)	5.8 (2)	0.0 (9)	−3.0 (5)	0.0 (0)
Ca(1)	2.4 (9)	7.1 (8)	7.8 (10)	−0.3 (6)	0.0 (7)	0.7 (7)

[a] $\exp[-19.739(U_{11}hha^*a^*... + 2(U_{12}hka^*b^*...))]$.

(2) Torardi, C. C.; Parise, J. B.; Subramanian, M. A.; Gopalakrishnan, J.; Sleight, A. W. *Physica C* **1989**, *157*, 115.
(3) Gao, Y.; Lee, P.; Coppens, P.; Subramanian, M. A.; Sleight, A. W.; *Science* **1988**, *241*, 954.
(4) LePage, Y.; McKinnon, W. R.; Tarascon, J.-M.; Barboux, P. *Phys. Rev. B* **1989**, *40*, 6810.
(5) Ren, J.; Jung, D.; Whangbo, M.-H.; Tarascon, J.-M.; LePage, Y.; McKinnon, W. R.; Torardi, C. C. *Physica C* **1989**, *159*, 501.
(6) Conflant, P.; Boivin, J. C.; Thomas, D. *J. Solid State Chem.* **1976**, *18*, 133.
(7) Walker, N.; Stuart, D. *Acta Crystallogr.* **1983**, *A39*, 158.
(8) Calabrese, J. C., personal communication.

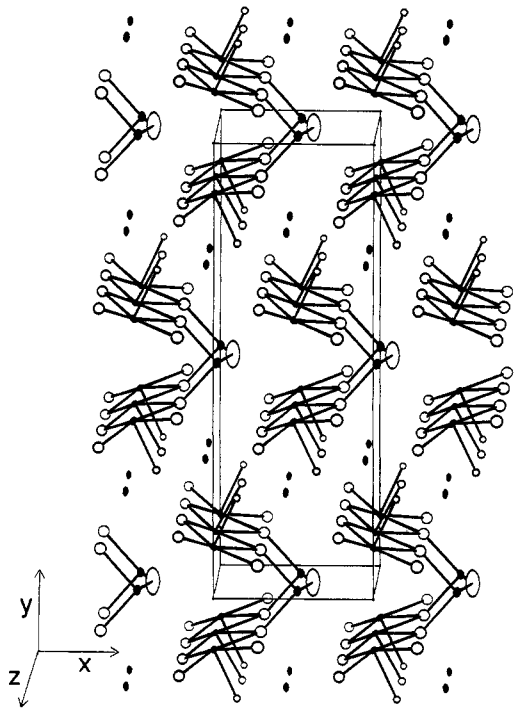

Figure 1. Structure of $Ca_4Bi_6O_{13}$ with atoms shown as 50% probability ellipsoids[16] (Tables II and III). Metal atoms are shaded. Only BiO bonds are shown, and O(2) atoms are on the average sites for clarity. Calcium ions are located at $y \sim {}^1/_4$ and ${}^3/_4$.

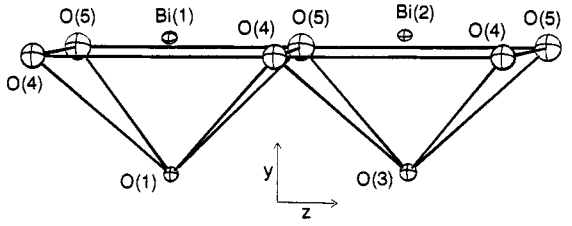

Figure 2. Coordination geometry of edge-shared Bi(1) and Bi(2) square pyramids in $Ca_4Bi_6O_{13}$.

parameter (2.6 to 1.2 Å^2) was obtained[9] when this atom was "split" by moving it to the 4e sites (x, y, ${}^1/_2$). The strongest peak in a final difference Fourier was 2.8 e/Å^3, located 0.92 Å from Bi(2) at the base of the square pyramid. Atomic parameters are given in Tables II and III. The absence of a center of symmetry was confirmed by the observation of a second harmonic signal, approximately 60 times that of quartz, in a specimen of the equilibrated powder.

Results and Discussion

With the formal oxidation states of Ca^{2+} and O^{2-}, the average oxidation state of Bi in $Ca_4Bi_6O_{13}$ is +3, so that each Bi center is expected to carry a pair of electrons in a lone-pair orbital. This orbital is largely made up of the Bi 6s orbital but includes some Bi 6p orbital character such that it extends away from the surrounding oxygen atoms. Although this lone-pair orbital has hybrid character, it will be simply referred to as the Bi 6s lone pair.

The structure of $Ca_4Bi_6O_{13}$ (Figure 1) is composed of double ribbons of edge-shared BiO_5 square-based pyramids (Figure 2), linked by Bi_2O_5 groups (Figure 3) and oriented in the c-axis direction. Sheets of these c-shaped double ribbons, which are parallel to (010), are separated by the calcium ions in monocapped trigonal prismatic coordination with oxygen. Those open parts of the structure

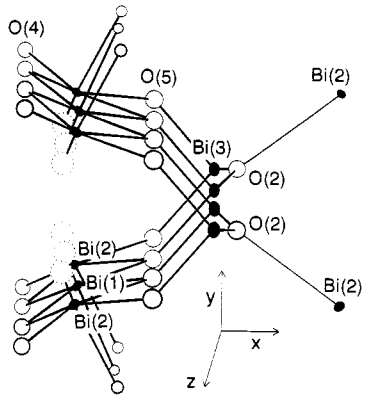

Figure 3. Diagram showing the linking of Bi(1) and Bi(2) units in $Ca_4Bi_6O_{13}$ (Figure 2) to form chains in z that are linked along y by three-coordinate Bi(3). One of each pair of the half-occupied sites for O(2) is shown. Note the almost trigonal-planar geometry about these sites (see text). The 6s lone electron pairs can be envisioned pointing into the open parts of the structure, and a possible arrangement for Bi(1) and Bi(2) is suggested in the diagram by the dotted circles.

(Figure 1) are occupied by the Bi(1) and Bi(2) 6s lone-pair electrons pointing out of the base of the square pyramids. Each BiO_5 unit (Figure 2) shares trans basal edges, containing O(4) and O(5) atoms, to form the ribbons of alternating Bi(1)O and Bi(2)O pyramids in the c-axial direction. Both Bi(1) and Bi(2) atoms are displaced out of the basal plane, away from the apical oxygen atoms O(1) and O(3), respectively (Figure 2). The Bi(2) atom is displaced further from its square-pyramidal base (Figure 2) than the Bi(1) atom, suggesting some bonding interaction between Bi(2) and O(2) (vide infra) (Figure 3). The ribbons formed by Bi(1) and Bi(2) are linked by $Bi(3)O_3$ groups.

The unusual coordination about Bi(3) is pyramidal with three short BiO bonds (2.01–2.06 Å). Along the c direction, the Bi(3) and O(2) atoms form ···BiOBi···BiOBi··· chains, in which the Bi···Bi contacts are short, 3.341 (2) Å. Unlike the Bi 6s lone pairs of the Bi(1) and Bi(2) centers, therefore, those of the Bi(3) centers are expected to strongly overlap and hence lead to significant destabilization (i.e., two-orbital four-electron destabilization).[10] When the O(2) atom is moved from the 2b to the 4e sites, it is displaced by about 0.25 Å from the center of the Bi(3)O(2)Bi(3) bridge (of the 2b setting) in the direction perpendicular to the bridge. This displacement makes the O(2) atom closer to Bi(2), 2.87 Å, and the geometry around O(2) becomes trigonal planar (Figure 3). (The sum of the three Bi–O(2)–Bi bond angles is 359.5°.) This geometry and the short Bi(3)–O(2) bonds suggest the presence of substantial π-bonding in the Bi(3)–O(2) bonds, which is consistent with the finding that the bond valence sums of Bi(3) and O(2) are quite large (3.4 and 2.6, respectively).[11]

Without the O(2) atom displacement (from the 2b setting, see Table II), only the Bi $6p_x$ and $6p_z$ orbitals can mix with the Bi 6s orbital to make up the Bi lone-pair orbital, so that two Bi lone-pair orbitals associated with each Bi···Bi contact are contained in the xz plane (see Figure 4). When the O(2) atom is displaced, the mirror plane symmetry of the local Bi(3) environment is lost. Thus, the Bi $6p_y$ orbital can also mix into the Bi lone-pair orbital. An important consequence of this Bi $6p_y$ orbital mixing is to tilt the resulting Bi lone-pair orbital away from the xz plane. This lone-pair tilting would make smaller the lone pair–lone pair

(9) Hamilton, W. C. *Acta Crystallogr.* **1965**, *18*, 502.

(10) Albright, T. A.; Burdett, J. K.; Whangbo, M.-H. *Orbital Interactions in Chemistry*; Wiley: New York, 1985.

(11) Brown, I. D.; Altermatt, D. *Acta Crystallogr.* **1985**, *B41*, 244.

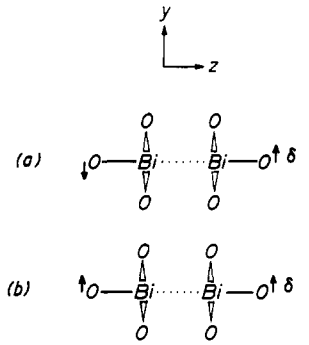

Figure 4. Schematic representations of the $(O_3Bi\cdots BiO_3)^{6-}$ clusters in $Ca_4Bi_6O_{13}$ employed for molecular orbital calculations to examine the lone-pair interactions between the Bi(3) atoms, where the dotted lines refer to the Bi(3)···Bi(3) contacts along the crystallographic c direction. The O(2) atoms are displaced by δ (Å) in the opposite directions in (a) and in the same direction in (b).

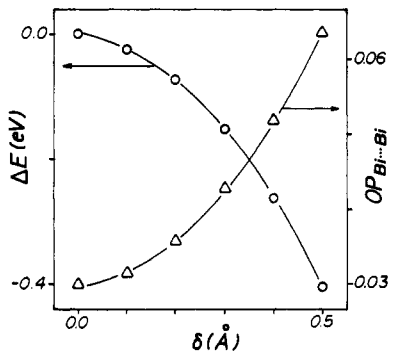

Figure 5. Energy lowering ΔE (eV) and Bi···Bi overlap population ($OP_{Bi\cdots Bi}$) of the $(O_3Bi\cdots BiO_3)^{6-}$ cluster in $Ca_4Bi_6O_{13}$ calculated as a function of the O(2) displacement δ (Å) by using the cluster model of Figure 4a. The energy lowering ΔE is measured with respect to the energy of the cluster for $\delta = 0$.

overlap in each Bi···Bi contact and hence reduce the lone pair–lone pair overlap destabilization. To verify this point, we performed extended Hückel[12,13] molecular orbital calculations on the $(O_3Bi\cdots BiO_3)^{6-}$ cluster as a function of the O(2) atom displacement δ (see Figure 4). The O(2) atoms of the $(O_3Bi\cdots BiO_3)^{6-}$ cluster are displaced in the opposite and same directions in Figure 4, parts a and b, respectively. Our computational results from the two displacement models are nearly identical, so we describe only those obtained from the model of Figure 4a. The HOMO of the $(O_3Bi\cdots BiO_3)^{6-}$ cluster is given by the antibonding combination of the Bi 6s lone-pair orbitals of the two BiO_3^{3-} fragments. As summarized in Figure 5 (ΔE vs δ), the energy of the $(O_3Bi\cdots BiO_3)^{6-}$ cluster is lowered as the displacement δ increases. The energy lowering, measured with respect to the energy of the cluster for $\delta = 0$, is very close to the value estimated from the HOMO energy lowering (i.e., twice the HOMO energy lowering). Thus the ΔE vs δ plot shows that with increasing δ, the overlap between the Bi 6s lone pair orbitals in the Bi···Bi contact decreases, thereby reducing the lone pair–lone pair overlap destabilization. A decrease in the extent of antibonding in the HOMO of the $(O_3Bi\cdots BiO_3)^{6-}$ cluster enhances the overlap population of the Bi···Bi contact. Thus, as shown in Figure 5, the Bi···Bi overlap population increases with increasing the displacement δ.

Table IV. Interatomic Distances (Å) and Angles (deg) for $Ca_4Bi_6O_{13}$[a]

Bi(1)–O(1)	2.059 (11)	Ca(1)–O(1)f	2.532 (8)
Bi(1)–O(4)a	2.333 (8) (×2)	Ca(1)–O(1)e	2.467 (8)
Bi(1)–O(5)a	2.437 (8) (×2)	Ca(1)–O(3)f	2.505 (8)
Bi(2)–O(3)	2.082 (12)	Ca(1)–O(3)	2.460 (8)
Bi(2)–O(4)	2.220 (8) (×2)	Ca(1)–O(4)h	2.476 (9)
Bi(2)–O(5)	2.601 (8) (×2)	Ca(1)–O(4)g	2.346 (9)
Bi(2)–O(2)k	2.866 (23)	Ca(1)–O(5)	2.357 (10)
Bi(3)–O(2)	2.013 (6)		
Bi(3)–O(5)l	2.064 (9) (×2)		
O(1)–Bi(1)–O(4)a	87.0 (3)	O(3)–Bi(2)–O(4)	87.8 (3)
O(1)–Bi(1)–O(5)a	81.9 (3)	O(3)–Bi(2)–O(5)	78.9 (3)
O(4)a–Bi(1)–O(4)b	105.6 (4)	O(4)–Bi(2)–O(4)i	103.7 (4)
O(4)a–Bi(1)–O(5)b	166.5 (3)	O(4)–Bi(2)–O(5)i	166.1 (3)
O(4)a–Bi(1)–O(5)a	81.5 (3)	O(4)–Bi(2)–O(5)	80.1 (3)
O(5)a–Bi(1)–O(5)b	89.3 (4)	O(5)–Bi(2)–O(5)i	93.3 (4)
O(2)–Bi(3)–O(5)m	93.2 (7)		
O(2)–Bi(3)–O(5)l	103.8 (7)		
O(5)l–Bi(3)–O(5)m	97.4 (5)		

[a] a, $-1/2+x$, $1/2-y$, $1-z$; b, $-1/2+x$, $1/2-y$,$-1+z$; c, $-1+x$, y, $-1+z$; d, $-1+x$, y, $1-z$; e, $1+x$, y, $1+z$; f, $1/2+x$, $1/2-y$, $1-z$; g, $1+x$, y, z; h, $1/2+x$, $1/2-y$, z; i, x, y, $1-z$; j, $-1/2+x$, $1/2-y$, z; k, x, $1-y$, $1-z$; l, $-1+x$, y, z; m, $-1+x$, $1-y$, z; n, x, $1-y$, $2-z$.

The above discussion strongly suggests that the O(2) atom displacement is a way of reducing the extent of the lone pair–lone pair overlap destabilization in the short Bi(3)···Bi(3) contacts. According to the ΔE vs δ plot of Figure 5, the O(2) displacement of $\delta \approx 0.25$ Å lowers the energy of $Ca_4Bi_6O_{13}$ by about 2.5 kcal/mol per Bi···Bi contact.

Conclusion

The structural consequence of the stereochemically active lone pair of electrons associated with Bi^{3+} is clearly illustrated in $Ca_4Bi_6O_{13}$. The concept that lone pairs, associated with Sb^{3+}, Bi^{3+}, and Pb^{2+}, are found in positions that are normally occupied by anions has been used in a number of studies[14] to rationalize and compare structural features unique to compounds containing these ions. For $Ca_4Bi_6O_{13}$, the lone pair of electrons can be considered to occupy the vacant octahedral sites of the coordination polyhedra about Bi(1) and Bi(2), opposite O(1) and O(3), respectively (Figure 2). This gives rise to a tunnel along the c-axial direction in the structure with ribbons forming the floor and ceiling and Bi(3)O(2)Bi(3) units the walls (Figure 3). The long Bi(2)–O(2) distance (Table IV) is a consequence of the repulsion between O(2) and the Bi(2) lone pair.

The Bi(3)···Bi(3) contacts of 3.341 (2) Å are surprisingly short when one takes into account the fact that the Bi 6s lone-pair orbitals are angled toward each other, so that the lone pair–lone pair overlap destabilization of each Bi(3)···Bi(3) contact is relatively large. Our molecular orbital calculations suggest that the O(2) atom displacement, in the direction perpendicular to the Bi(3)O(2)Bi(3) bridge, is a way of reducing the overlap destabilization in each Bi(3)···Bi(3) contact. This energy lowering, which is calculated to be ~2.5 kcal/mol per Bi···Bi contact at the O(2) displacement δ of ~0.25 Å, is not large. Therefore, it is probable that the O(2) atom displacement is not static.

It is of interest to note that the pyramidal $Bi(3)O_3$ units of $Ca_4Bi_6O_{13}$ are very similar to those found in the new superconductors such as $Bi_{2-x}Pb_xSr_2CuO_6$[15] and Bi_2Sr_2-

(12) Hoffmann, R. *J. Chem. Phys.* **1963**, *39*, 1397.

(13) The atomic parameters of Bi and O employed in our work are taken from ref 5, except that d functions of Bi are omitted in the present calculations. The off-diagonal elements of the extended Hamiltonian, H_{ij}, were calculated by using the modified Wolfsberg–Helmholz approximation; see: Ammeter, J. H.; Burgi, H.-B.; Thibeault, J.; Hoffman, R. *J. Am. Chem. Soc.* **1978**, *100*, 3686.

(14) See, for example: Andersson, S.; Astrom, A. *Solid State Chemistry Proceedings of the 5th Materials Research Symposium*; Roth, R. S., Schneider, S. J., Eds.; NBS Special Publication 364; National Bureau of Standards, Washington, DC, 1972; pp 3–14.

(15) Torardi, C. C.; McCarron, E. M.; Parise, J. B., to be published.

$CaCu_2O_8$.[2] These layered compounds have double bismuth oxide layers in which the Bi lone pairs are oriented between the two BiO sheets thus imparting a micaceous morphology.

(16) Johnson, C. K. ORTEP: *A Fortran Thermal-Ellipsoid Plot Program for Crystal Structure Illustration*; Oak Ridge National Laboratory Report 5138, 1976.

Acknowledgment. The technical assistance of W. J. Marshall for the X-ray data collection, C. R. Miao for syntheses, and M. A. Saltzberg and S. C. Winchester for DSC measurements is acknowledged.

Supplementary Material Available: A listing of structure factor amplitudes (5 pages). Ordering information is given on any current masthead page.

Luminescence Efficiency of Ions with Broad-Band Excitation in Lithium Lanthanum Phosphate Glass

J. W. M. Verwey* and G. Blasse

Debye Research Institute, University of Utrecht, P.O. Box 80,000, 3508 TA Utrecht, The Netherlands

Received March 12, 1990

The luminescence of several ions in lithium lanthanum phosphate glass is investigated and compared with the luminescence of these ions in lanthanum borate glass. The efficiency of the luminescence is much higher in the phosphate glass. For some ions a comparison with their luminescence in crystalline $LiLaP_4O_{12}$ is also made. The results lead to some conclusions about the influence of the host material on the luminescence efficiency. These results are discussed, and examples are used to illustrate these conclusions.

Introduction

In a previous paper the authors reported the luminescence efficiency of several ions in lanthanum borate (LaB_3O_6) glass and in crystalline LaB_3O_6.[1] The luminescence efficiency for excitation into broad bands was much lower in the glass than in the crystals. A single configurational coordinate (scc) model was used to explain the different luminescence efficiencies of these ions in both modifications. However, the trends and rules noted in that study were proven valid only for the crystalline borate and glass modifications, so it seemed worthwhile to investigate whether they are also valid in a different host. Lithium lanthanum phosphate ($LiLaP_4O_{12}$) is a logical choice due to the following reasons: (a) The crystalline material has been studied intensively because of its possibilities as a stoichiometry laser material;[2,3] (b) efficient broad-band luminescence has been reported for several activators in the crystalline modification;[4] (c) phosphate glasses are investigated and used for high average power (hap) lasers;[5] (d) to our knowledge, there has been only one comparison of the luminescence in the glassy and crystalline modifications for Nd^{3+}–Yb^{3+} energy transfer in $LiLaP_4O_{12}$.[6] Only the narrow $4f^n$ transitions were studied here.

In this paper we report a luminescence investigation of several ions with broad-band excitation transistions in lithium lanthanum phosphate crystals and glasses. The luminescence efficiency is, generally speaking, higher than that for the borate glass. By examining the differences in the spectra, we are able to determine the influence of the nature of the host material on the luminescence of the ions. It will be shown that by using the scc model, it is possible to predict qualitatively the luminescence efficiency of doped glasses.

Experimental Section

Preparation. The starting materials for the preparation of the lithium lanthanum phosphate (LLP) glasses are $NH_4H_2PO_4$, Cr_2O_3, and Li_2CO_3 (Merck p.a), Bi_2O_3 (Baker), and the rare-earth oxides La_2O_3, CeO_2, Pr_4O_{11}, Eu_2O_3, Gd_2O_3, and Tb_4O_7 (Highways International, 5N). The dopant concentration is ~1 mol %. Due to the volatility of phosphorus pentoxide, an excess of 10–12% $NH_4H_2PO_4$ was added to the stoichiometric mixture before melting. This mixture is heated for 2 h at 250 °C and 3 h at 550 °C. When most of the H_2O and NH_3 have been evaporated, the mixture is melted in a quartz crucible at 1270 °C for ~30 min. The glasses containing Ce^{3+}, Pr^{3+}, or Tb^{3+} are melted under a N_2/H_2 mixture (4:1). The glasses are poured into a carbon mould at 470 °C and cooled to room temperature at a rate of 1 °C/min. Crystalline samples of composition $LiLa_{1-x}M_xP_4O_{12}$ (M = Ce^{3+}, Eu^{3+}, Tb^{3+}, Bi^{3+}) are prepared according to the literature.[4,7,8] They are checked by X-ray powder diffraction and infrared spectroscopy.[8] The results show these samples to be single phase.

Optical Measurements. Luminescence spectra were measured on powdered samples and on polished glass samples of 6 × 6 × 10 mm. Measurements were carried out at various temperatures ranging from 4.2 to 300 K. Emission and excitation spectra were recorded with a Perkin-Elmer MPF 3L spectrofluorometer equipped with an Oxford Instruments helium flow cryostat. The spectra were corrected for the lamp intensity and the transmittance of the monochromator with the use of Lumogen T-rot G.G as a standard.[9] For excitation wavelengths shorter than 240 nm, the setup described in ref 10 was used. Diffuse reflection spectra of the powdered samples were recorded at room temperature with a Perkin-Elmer Lambda 7 UV/vis spectrophotometer. The same apparatus was used to measure the absorption spectra of 6-mm-thick glass samples. The absorption spectra were not corrected for reflectance losses. The luminescence efficiency is determined by comparison with standard phosphors.

(1) Verwey, J. W. M.; Blasse, G. *Mater. Chem. Phys.* **1990**, *25*, 91.
(2) Krühler, W. W.; Jeser, J. P.; Danielmeyer, H. G. *Appl. Phys.* **1973**, *2*, 329.
(3) Danielmeyer, H. G.; Weber, H. P. *IEEE J. Quantum Electron.* **1973**, *QE-8*, 805.
(4) Blasse, G.; Dirksen, G. J. *Phys. Status Solidi B* **1982**, *110*, 487.
(5) Marion, J. E. Advanced phosphate glasses for high-average-power lasers, Glasses for Optoelectronics. *Proc. SPIE.* **1989**, *1128*, 318.
(6) Parent, C.; Lurin, C.; LeFlem, G.; Hagenmuller, P. *J. Lumin.* **1986**, *36*, 49.
(7) Moktar, M. F.; Ariguib, N. K.; Trabelsi, M. *J. Solid State Chem.* **1981**, *38*, 128.
(8) Rzaigni, M.; Ariguib, N. K. *J. Solid State Chem.* **1981**, *39*, 128.
(9) Bril, A.; de Jager-Veenis, A. W. *J. Res. NBS* **1976**, *80A*, 401.
(10) Verwey, J. W. M.; Dirksen, G. J.; Blasse, G. *J. Non-Crystalline Solids* **1988**, *107*, 49.

0897-4756/90/2802-0458$02.50/0